COMPARATIVE STUDY OF K-NN, NAÏVE BAYES AND SVM METHODS FOR BUILDING COLLAPSE DETECTION USING IMAGE FEATURES

Mehdi Rezaeian*[1] and Armin Gruen[2]
[1] Assistant Professor, Electrical and Computer Engineering Department, Yazd University
Daneshgah Blvd., Safa-ieh, Yazd, Iran; Tel: +98-351-8122610
E-mail: mrezaeian@yazduni.ac.ir

[2] Professor, Institute of Conservation and Building Research, ETH Zurich
Wolfgang-Pauli-Strasse 27, CH-8093 Zuerich Switzerland; Tel: +41-44-6333038
E-mail: armin.gruen@geod.baug.ethz.ch

KEY WORDS: Supervised classification, Collapse detection, Earthquake.

ABSTRACT: After an earthquake, the image-based interpretation methods are powerful tools for detection and classification of damaged buildings. In this paper several methods for extracting imagery features are examined. Experiments are performed on two datasets of the Kobe and Bam earthquakes. We use only the post-earthquake images and the pre-earthquake images are not needed. The regions of interest are delineated with the aid of prismatic models of buildings. First and second order statistical descriptors including standard deviation, entropy and homogeneity are evaluated. They are computed for small windows around pixels and average values were assigned to each building polygon. The assessments show that this kind of descriptors are less sensitive to soft damage and suffer from miscellaneous textures in high-resolution images in urban area. We propose "Regularity indices" to describe the appearance of the building as regular or irregular. Regularity indices were defined by taking account of lines composition with regards to building footprint. Three kinds of classification methods: k-NN, naïve Bayes and support vector machine (SVM) are used and compared. The implemented program extracts all attributes including statistical features (average standard deviation, average entropy and homogeneity) and regularity indices for any building polygon. Numerical results revealed fairly good performance of the proposed features for collapse detection. The classification results are evaluated by a cross-validation method and by an independent visual interpretation test set. The results achieved with Bayesian and SVM classifier are better than with the 3-NN classifier.

1. INTRODUCTION

After an earthquake, demolished structures have to be recorded in order to give a map of buildings damage and property losses. Photo-interpretation analysis can be a reliable technique for earthquake damage assessment, depending on the objectives and the image resolution. Large-scale images show certainly the high level of details related to single buildings and small structures and the human interpreter is able to look for the remaining ruins and debris from damaged buildings. Automation could be a way for eliminating the time-consuming procedures, which are usually carried out by human operators. Change detection techniques can be employed to detect "significant" changes while rejecting "insignificant" ones. However, it is necessary to define specific criteria to define how a 'change' is translated to 'damage'. For this purpose, pictorial attributes like edges, texture or shadows can be extracted. For instance, the presence/absence of shadows in a pre/post event pair is a signal of a collapsed building (Turker & San, 2004, Vu et al. 2004b, Turker and Sumer 2008) and texture analysis can be conducted for debris detection (Sumer and Turker 2005, Rehor and Vögtle 2008). The presence and amount of debris can be translated to damaged structures and rate of its demolition. The type of debris in terms of its material, shape and formation is generally complex and its reflectance characteristics can be very different in images. Nevertheless, the image descriptors, which provide measures of properties such as smoothness, coarseness and regularity, can intuitively be utilized for debris detection. However, there is no clear definition of "debris texture" and it is often qualitatively characterized by its coarseness in the sense that a patch of rubbles is coarser than a patch of intact building roof under the same viewing condition. Various approaches have been used to investigate the textural and spatial structural characteristics of image data for damage detection, including first and second order statistical features, wavelet transform, morphological descriptors, variograms and density or dissimilarity of edge pixels (Rathje et al. 2005, Shirzaei et al. 2006, Sertel et al. 2007, Rehor and Vögtle 2008, Rezaeian & Gruen 2011a).

Our goal in this paper is to generate appropriate features and comparing classification methods for detection of damaged buildings. In this approach, after extracting the building position from vector maps, by measuring and comparing different textural features for extracted buildings in both pre- and post-event images, building conditions are extracted. Three kinds of classification methods: k-NN, naïve Bayes and support vector machine (SVM) are used and compared.

2. IMAGE FEATURES

2.1 Image preparation

Two datasets were obtained from aerial images. In our research, parts of the Kobe and Bam cities are selected as study regions. The calibration reports of the cameras and ground control points were available and used as input information for the interior and exterior orientation procedures. A visual inspection of building damages was conducted, based on stereo pairs of aerial photos to generate reference data and for extracting prismatic model of buildings. The test regions encompass 637 and 890 houses in Kobe and Bam cities, respectively.

Furthermore, we apply an adaptive histogram equalization technique in which histograms are generated only at a rectangular grid of points and the mappings at each pixel are generated by interpolating mappings of the four nearest grid points (Gonzalez and Woods 2002). In addition, optical images which are taken just after an earthquake are subject to noise and haze of dust and smoke. Debris pattern generally contains high-frequency components and it is so difficult to distinguish from noise added to image, which similarly has a high spatial frequency spectrum. Since linear low-pass filtering may degrade feature generation results, the images are smoothed only with a 3by3 non-linear median filter in order to limit impulse noise effects.

2.2 Features generation

2.2.1 Statistical descriptors: First, we select the following descriptors as quantitative measures:

$$\text{Standard Deviation: } SD = \left[\sum_{b=0}^{L-1} (b-\bar{b})^2 P(b)\right]^{1/2} \qquad \text{Entropy: } E = -\sum_{b=0}^{L-1} P(b)\log_2 P(b) \tag{1}$$

The first order histogram estimate ($P(b)$, b represents quantized amplitude gray-level) is simply computed in a neighborhood window centered about (i,j). The standard deviation is a measure of gray-level contrast that can be used to represent relative smoothness. Entropy is a measure of histogram uniformity. The closer to the uniform distribution ($P(b)$=constant) the higher the E. For every point within the building area, small windows around the points are selected and standard deviation and entropy are computed. Also, Haralick et al. (1973) have proposed a number of texture features based on the two-dimensional histogram of pixel pairs ($P(b_{i},b_{j})$). For our purpose, the following useful descriptor is selected to:

$$\text{Homogeneity: } \qquad H = \sum_{i,j}^{L-1} \frac{P(b_i, b_j)}{1+|i-j|} \tag{2}$$

'H' returns a value that measures the closeness of elements to the diagonal matrix ('H' is 1 for a diagonal matrix). In order to analysis the texture of building image, average standard deviation (ASD) and average entropy (AE) together with homogeneity are computed and assigned to each building polygon.

2.2.2 Regularity indices: For the purpose of improving the classification of building damage types, especially to detect debris and rubbles, we present two kinds of features using linear features. Direction, interconnection and clarity of lines may be key signal for human perception to discern devastated structures. The main characteristic feature for uncollapsed building can be the well-ordered distinct lines and their "regularity". The degree of geometric regularity, not only at the building level itself but also at higher levels of spatial hierarchy can also be exploited. To measure "lines regularity" we define criteria that give a numerical index.

Line detection of standing buildings exhibits a sketchy outlines draft. The composition of lines could be a remarkable cue of scene regularity. Here, regularity might be defined based on line directions with respect to the predefined building model. Regularity indices are defined for exterior and interior zones: the narrow strip around the border of building and the region surrounded by building polygon (Figure 1). At the border of the building polygon, the output lines are compared with vector lines, which being already extracted from pre-event images. In order to evaluate the degree of fit of line segments to the pre-defined polygons two parameters were used: 1) the angle between segmented lines and actual polygon lines (α) 2) the length of segmented lines (l). To measure the degree of the match between the detected segment lines and delineated vectors of building polygons, the following formula is established for the first regularity index:

$$RI_1 = f\left(\frac{\sum l_i \cos\alpha_i}{\sum l_i}\right) \tag{3}$$

The function *f* describes the rate of fit between detected line segments and actual polygon lines. The second regularity index (RI2) is defined based on density of line segments. For this index, those lines within building polygon which their direction are not close to the direction of polygon lines would be selected and density of pixels is calculated (Figure 1). In comparison with the conventional statistical features, regularity indices show better results.

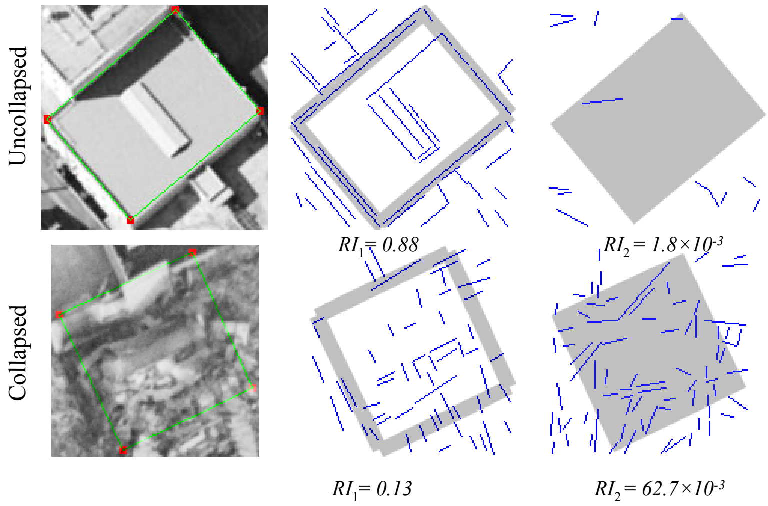

Figure 1: Regularity indices (RI_1, RI_2) are computed for exterior and interior regions

2.3 Features evaluation

In this section, the performances of proposed features are evaluated using a figure-of-merit method by "Fisher discriminant ratio" (FDR) and "B-distance" criteria (Theodoridis & Koutroumbas 2003). The values of the criteria are computed for each of the features and then are ranked in order of descending values. The best values can describe the classification effectiveness of individual features or feature vectors. Features of potential interest include the average standard deviation (ASD), average entropy (AE), homogeneity (H) and the proposed regularity indices (RI_1, RI_2). These features are computed for each one of the building polygons from the reference data ("Collapsed" and "Uncollapsed" visually classified buildings). Fisher discriminant ratio and one-dimensional B-distance measurements of these imagery features are calculated and presented in Table 1.

Table 1: FDR and B-distance of proposed features for bi-level classification ("Collapsed" and "Uncollapsed")

Kobe data set					
	RI_2	RI_1	H	AE	ASD
FDR	2.43	1.96	1.06	0.75	0.73
B-distance	0.68	0.50	0.30	0.24	0.18
Bam data set					
	RI_1	RI_2	ASD	AE	H
FDR	1.10	0.89	0.68	0.15	0.05
B-distance	0.35	0.23	0.17	0.10	0.04

In this table the discrimination properties of individual features are presented. Both B-distance and FDR measurements indicate that the regularity indices are marginally more effectual separators for "Collapsed" and "Uncollapsed" buildings categories. In Bam city most buildings were made of clay bricks, and resulting textural features are not robust separators, although using boundary feature (RI_1) yields the best result with the largest B-distance.

3. AUTOMATIC COLLAPSE DETECTION USING POST-EVENT IMAGERY DATA

Figure 2 depicts a flowchart of operations for collapse detection using imagery features. Here, we use only the post-earthquake images and the pre-earthquake images are not needed. The regions of interest are delineated with the aid of prismatic model of buildings. The implemented program extracts all attributes including statistical features (average standard deviation, average entropy and homogeneity) and regularity indices for any building polygon.

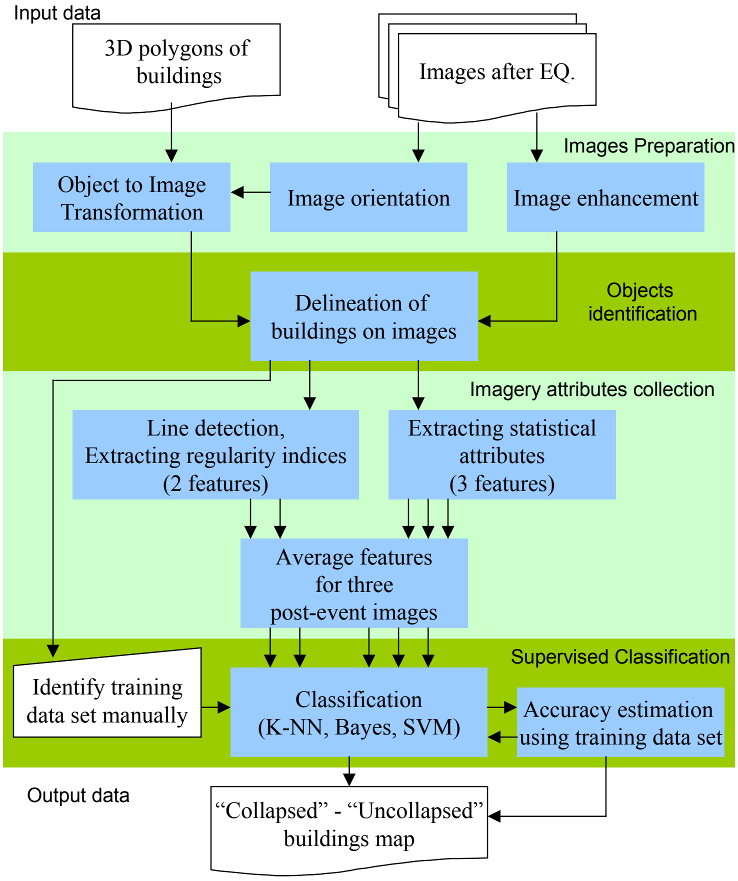

Figure 2: The processing flowchart collapse detection using post-event imagery features

The variables resulting from this procedure are calculated for a triplet set of post-event aerial images and final normalized features are generated from average values. Our study compares three classification methods (k-Nearest Neighbors, Bayesian and Support Vector Machines) for the production of collapse maps from aerial images.

After performing the classification, it is important to evaluate the quality of the results. The ideal process is to have an independent set of test data. The training data split into two sets: one to be used for training and the other for validation. The classification results were evaluated by a cross-validation method and by an independent visual interpretation test set. We used *random sub-sampling validation* technique. This method randomly splits the dataset into training and validation data. For each such split, the classifier is retained with training data and validated on the remaining data. The process is repeated for each of the subsets as validation. The error matrix from each split can then be averaged. In this method all observations are used for both training and validation. The goal of cross-validation is to estimate the expected level of accuracy to a data set that is independent of the data that were used to train the model. Primarily, a bi-level classification is tested in order to generate a map of "Collapsed" and "Uncollapsed" buildings.

The procedures of image enhancement and orientation are performed by commercial software but features extraction - especially line detection algorithm (Hierarchical Permissive Hough Transform) - are implemented with customized codes (Rezaeian & Gruen 2011b). We used combination codes of C++ and Matlab (ver. 7.4.0 R2007a) to implement the described procedures in Figure 2. Statistical features as well as the second regularity index (RI_2) are calculated only for pixels within building polygons so that only roof textures are employed for classification. However, the first regularity index (RI_1) looks for intact lines around the building footprint. Therefore, the collapsed buildings such as "pancake" and "overturned" that shifted from initial position can be detected using this attribute (RI_1).

4. NUMERICAL RESULTS AND DISCUSSION

The k-nearest neighbor classifier was conducted with Euclidian distance metric. A direct majority vote from the nearest three neighbors (k = 3) was employed. The experiments showed that the performance of k-NN was not sensitive to the exact choice of k when k was large. Although for small values of k, the k-NN algorithm was more robust than the 1-NN algorithm. We used a linear form of Bayesian classifier using a pooled estimate of covariance matrix. The experiments showed that for our data set there is no significant preference between quadratic or linear form of this classifier. The major advantage of the naïve Bayes classifier is its short computational time for training. We used Matlab ready functions for SVM classification using a linear kernel. For training, a Sequential Minimal Optimization (SMO) method is conducted. SMO is a simple algorithm, which is conceptually incomplex, easy to implement without any extra matrix storage and without using numerical quadratic programming optimization at all.

Table 2 present average error matrix and accuracy assessments for the three classifiers: 3-NN, Bayesian and SVM. Sample buildings (fifteen buildings for each class) were acquired as a training set. Validations are performed 100 times each time with new training data set for obtaining average values of error matrix components.

Table 2: Average error matrix of 100 times cross validation for collapse detection using image features

Input data: post-event aerial images + building polygons	Visual interpretation			
	Kobe		Bam	
3-NN classifier	Uncollapsed	Collapsed	Uncollapsed	Collapsed
Uncollapsed	247	51	333	119
Collapsed	30	309	75	363
Overall accuracy	**87.3%**		**78.2%**	
Bayesian classifier	Uncollapsed	Collapsed	Uncollapsed	Collapsed
Uncollapsed	241	35	340	123
Collapsed	36	325	68	359
Overall accuracy	**88.9%**		**78.5%**	
SVM classifier	Uncollapsed	Collapsed	Uncollapsed	Collapsed
Uncollapsed	244	36	342	116
Collapsed	33	324	66	366
Accuracy Assessment - SVM classifier				
Overall accuracy	**89.2%**		**79.6%**	

The results achieved with Bayesian and SVM classifier are better than with the 3-NN classifier. While the Bayesian classifier performed faster on the learning process, the SVM classifier is faster in the classification process. The advantage of Bayesian classifier is the facility to build the classifier. The basic k-NN has usually only a single parameter (k), which is relatively easy to tune. Although the SVM shows better overall accuracy, it has more parameters than other techniques and the process of training in SVM classifier is more complicate. The size of the training set has to be sufficiently large. Table 3 shows results of using different sizes of training data sets for the Bayesian classifier. In fact, employing large number of buildings as training data increase the accuracy as well as reliability of classifier. Also, using more training data causes difference between the actual accuracy and estimated accuracy - calculated based on the training data set - to be decreased. Our experiments revealed that for both the Kobe and Bam datasets minimum fifteen buildings per each class could be suitable for training procedure.

Table 3: Average overall accuracies (± std.) and difference between actual and estimated values of 100 times cross-validation for various sizes of training sets

Bayesian classifier		Number of buildings selected as training set for each class					
		5	10	15	30	60	100
Kobe	Overall accuracy	%81±7	%87±3	%89±2	%90±1	%90±1	%91±1
Kobe	Average difference between estimated accuracy and actual accuracy	%16.5	%8.3	%4.9	%2.1	%1.2	%0.3
Bam	Overall accuracy	%70±9	%78±4	%79±2	%81±1	%82±1	%82±0.5
Bam	Average difference between estimated accuracy and actual accuracy	%24.4	%10.8	%5.0	%3.2	%1.0	%0.5

5. CONCLUSIONS

In the course of this research several methods for extracting imagery features were examined. First and second order statistical descriptors including standard deviation, entropy and homogeneity were evaluated. The assessments show that this kind of descriptors, measuring image amplitude in terms of luminance or tristimulus values, are less sensitive to soft damage and suffer from miscellaneous textures in high-resolution images in urban area. Texture is a neighborhood property of an image points and therefore, texture measures are inherently dependent on the image scale. We aimed to describe the look of building image as regular or irregular. Regularity indices were defined taking account of lines composition with regards to building footprint. Experimental results revealed fairly good performance of the proposed features for collapse detection. Three kinds of classification methods: k-NN, Bayesian and SVM were used and compared. The classification results were evaluated by a cross-validation method and by an independent visual interpretation test set. The Support Vector Machine (SVM) classifier is a relatively new method that proved to be quite effective for damage detection. One reason for erroneous categorized building is the absence of the imagery features in the area where the buildings are hidden in the shadows or occluded by other objects. Besides, for complex shapes building borderlines couldn't be matched exactly with building polygon. It is therefore impossible to find line segments corresponding to the line of the building polygon

6. REFERENCES

Gonzalez, R. C., Woods, R. E. (2002). Digital Image Processing - Second Edition. Prentice-Hall, Inc., New Jersey.

Haralick, R. M., Shanmugam, K., Dinstein, I. (1973). Textural fatures for image Classification. IEEE Transaction on systems, Man and Cybernetics, vol.3, no.6, pp. 610-621.

Rathje, E. M., Crawford, M., Wo, K., 2005. Damage Patterns from Satellite Images of the 2003 Bam, Iran, Earthquake. Earthquake Spectra, Volume 21, No. S1, S295–S307.

Rehor, M., Vögtle, T., 2008. Improvement of building damage detection and classification based on laser scanning data by integrating spectral information. International Archive of Photogrammetry and Remote Sensing (IAPRS), 37 (B7), pp. 1599-1605.

Rezaeian, M., Grün, A., 2011a. Automatic 3D building extraction from aerial and space images for earthquake risk management. Journal of Georisk (Taylor & Francis): Assessment and Management of Risk for Engineered Systems and Geohazards, 5(1), pp 77-96.

Rezaeian, M., Grün, A., 2011b. Image-based recognition and classification of damaged buildings using Bayesian network. GeoInformation for Disaster Management Conference, 3-8 May, Antalya, Turkey, 8p.

Sertel, E., Kaya, S., Curran, P.J., 2007. Use of Semivariograms to identify Earthquake Damage in an Urban Area. In: IEEE Transactions on Geoscience and Remote Sensing, Vol. 45, Issue 6, pp. 1590-1594.

Shirzaei, M., Mansouri, B., Shinozuka, M., 2006. Multiresolution Analysis of Satellite Optical Images for Damage Detection using Wavelet Transform. 4th International Workshop on Remote Sensing for Disaster Response, 25-26th, Cambridge, UK.

Sumer, E., Turker, M., 2005. Building Damage Detection from Post-Earthquake Aerial Imagery Using Building Grey-Value and Gradient Orientation Analyses. Proceedings of 2nd International Conference on Recent Advances in Space Technologies (RAST'05), Istanbul, Turkey, pp. 577-582.

Theodoridis, S., Koutroumbas, K. (2003). Pattern Recognition – Second edition. Elsevier, Academic Press, London, UK.

Turker, M., San, B. T., 2004. Detection of collapsed buildings caused by the 1999 Izmit, Turkey earthquake through digital analysis of post-event aerial photographs. Int. Journal of Remote Sensing, 25 (21), pp. 4701–4714.

Turker, M., Sumer, E., 2008. Building-based Damage Detection due to Earthquake using the Watershed Segmentation of Post-event Aerial Images. International Journal of Remote Sensing, Vol.29, No.11, pp. 3073-3089.

Vu, T. T., Matsuoka, M., Yamazaki, F., 2004. Shadow Analysis in Assisting Damage Detection Due to Earthquakes from Quickbird Imagery. International archives of Photogrammetry Remote Sensing and Spatial Information Sciences, 35 (7), pp. 607-610.